A comparison between different coronagraphic data reduction techniques

Carolo, E., Vassallo, D., Farinato, J., Bergomi, M., Bonavita, M., et al.

E. Carolo, D. Vassallo, J. Farinato, M. Bergomi, M. Bonavita, A. Carlotti, V. D'Orazi, D. Greggio, D. Magrin, D. Mesa, E. Pinna, A. Puglisi, M. Stangalini, C. Verinaud, V. Viotto, "A comparison between different coronagraphic data reduction techniques," Proc. SPIE 9909, Adaptive Optics Systems V, 99097Q (27 July 2016); doi: 10.1117/12.2232792

SPIE.

Event: SPIE Astronomical Telescopes + Instrumentation, 2016, Edinburgh, United Kingdom

A comparison between different coronagraphic data reduction techniques

Carolo E.[a,b], Vassallo D.[a,b,c], Farinato J.[a,b], Bergomi M.[a,b], Bonavita M.[d], Carlotti A.[e], D'Orazi V.[a,b], Greggio D.[a,b,c], Magrin D.[a,b], Mesa D.[a,b], Pinna E.[f,b], Puglisi A.[f,b], Stangalini M.[g,b], Verinaud C.[e], and Viotto V.[a,b]

[a]INAF - Osservatorio Astronomico di Padova, Vicolo dell'Osservatorio 5, 35122, Padova, Italy
[b]ADONI - Laboratorio Nazionale Ottiche Adattive, National Laboratory for Adaptive Optics, Italy
[c]Dipartimento di Fisica e Astronomia, Università degli Studi di Padova, Vicolo dell'Osservatorio 3, 35122, Padova, Italy
[d]Royal Observatory, Blackford Hill View, Edinburgh EH9 3HJ, United Kingdom
[e]Institut de Planétologie et d'Astrophysique de Grenoble, 414, Rue de la Piscine, Domaine Universitaire, 38400 St-Martin d'Hères, France
[f]INAF - Osservatorio Astrofisico di Arcetri, Largo Enrico Fermi 5, 50125 Firenze, Italy
[g]INAF - Osservatorio Astronomico di Roma, Via Frascati 33, 00078 Monte Porzio Catone, Roma, Italy

ABSTRACT

A robust post processing technique is mandatory for analysing the coronagraphic high contrast imaging data. Angular Differential Imaging (ADI) and Principal Component Analysis (PCA) are the most used approaches to suppress the quasi-static structure presents in the Point Spread Function (PSF) for revealing planets at different separations from the host star. In this work, we present the comparison between ADI and PCA applied to System of coronagraphy with High order Adaptive optics from R to K band (SHARK-NIR), which will be implemented at Large Binocular Telescope (LBT). The comparison has been carried out by using as starting point the simulated wavefront residuals of the LBT Adaptive Optics (AO) system, in different observing conditions. Accurate tests for tuning the post processing parameters to obtain the best performance from each technique were performed in various seeing conditions ($0.4" - 1"$) for star magnitude ranging from 8 to 12, with particular care in finding the best compromise between quasi static speckle subtraction and planets detection.

Keywords: SHARK-NIR, Coronagraphy, Exoplanets, ADI, PCA

1. INTRODUCTION

At the moment more than 3400 planets were discovered,[1] most of them have to be characterized, some also still to be confirmed. A coronagraphic imager with a high order adaptive optics correction is one of the most promising tools to detect, confirm, study and investigate on exoplanets.
A major drawback, when detecting the faint planets is represented by the noise due to the non common path aberration (NCPA) and the consequent generation of the quasi static speckles (QSS), in fact this noise pattern is hard to quantify for its space-random behaviour and its time-dependent nature.
An efficient post processing technique is mandatory for analysing the coronagraphic high contrast imaging data. ADI[2] and PCA[3] techniques are the most used approaches to suppress the quasi-static structure presents in the PSF for revealing planets at different separations from the host star. We present some preliminary results of ADI and PCA techniques applied to SHARK-NIR,[4] a coronagraphic camera which will be implemented at LBT.[5] The comparison has been carried out by using as starting point the simulated wavefront residuals of the LBT

Further author information: (Send correspondence to E.C.)
E.C.: E-mail: elena.carolo@oapd.inaf.it

Adaptive Optics Systems V, edited by Enrico Marchetti, Laird M. Close, Jean-Pierre Véran, Proc. of SPIE Vol. 9909, 99097Q

AO system,[6] in different observing conditions (thanks to the Arcetri AO team).This AO simulated data are then optical propagated by setting different coronagraphic configuration by an "ad hoc" IDL code explained in Ref. [7].

2. POST PROCESSING ANALYSIS

Accurate tests for tuning the post processing parameters to obtain the best performance from each technique were performed with various seeing conditions (0.4" − 1") for star R magnitude ranging from 8 to 12, with particular care in finding the best compromise between quasi static speckle subtraction and planets detection. In order to tune the amount of quasi static speckles, we compared detection limits for a sample of SPHERE[8] (the high contrast imager at VLT) data with SHARK simulations (in similar observing conditions) varying the level of noise, from 15 up to 60nm rms. The curves corresponding to SHARK simulations are placed within the detection range of SPHERE data. We take into account for the successive simulations 30nm rms because it is consistent with the numbers suggested via private communication by the Adaptive optics group involved in LUCI and LBTI alignment.
Different coronagraphic masks are taken into account for analysing the post processing data to estimate the instrument performance. In this document a selection of the tested masks are presented; a variant of the Classical Lyot Coronagraph[9] with a gaussian transmission focal plane (FP) mask (in the figures defined as GAUSS), a Gaussian Apodized Lyot Coronagraph[10] mask (in the figures defined as APLCG), with a Gaussian apodization of the first intermediate pupil and a variant of the Shaped Pupil (SP) Coronagraph,[11] that is a mask whose particular transmission pattern generates a high contrast region in the subsequent focal plane (in the figures defined as SPN4).

2.1 ADI: Angular Differential Imaging

The Angular Differential Imaging is a post processing technique used on direct imaging data to suppress the quasi-static structure present in the PSF.[12] The acquisition of a set of images (usually up to a few hundreds) is performed with the instrument rotator turned off. In this way the quasi-static PSF is stable during the observation while a rotation of the Field of View (FoV) with respect to the instrument occurs. Therefore, the planet (which may be confused with the speckles) rotates. For these simulations a simple version of the ADI technique is used (see Figure 1).

For the simple ADI version a reference PSF is obtained by taking the median of all images in the sequence and then subtracted to each image to remove the quasi-static structure. To mimic the real procedure, after the inclusion of fake planets in the simulated data-cubes, all the image differences are de-rotated to align the FoV and a final median is performed. A minimum FoV rotation of 30° is considered, in order to make sure that even at small angular separations the signal from the possible companion after the subtraction would be largely preserved.

2.2 PCA: Principal Component Analysis

We evaluated also the implementation of the PCA algorithm, that is based on a statistical representation of each frame in the data-cube as a linear combination of its principal orthogonal components. These components are estimated by diagonalizing the covariance matrix associated to the signal. Its application has been reported to be very effective particularly by manipulation of the number of principal components to maximize the signal from the planet near its host star.[13]
The number of modes used for the PCA analysis is associated to the variance of the corresponding principal component.
For both post processing algorithms the detection limits are calculated using the ratio of simulated planets peak intensities over the noise in the residual image as a function of the angular separation, to take into account the self-subtraction of the planet light due to the used post processing technique.

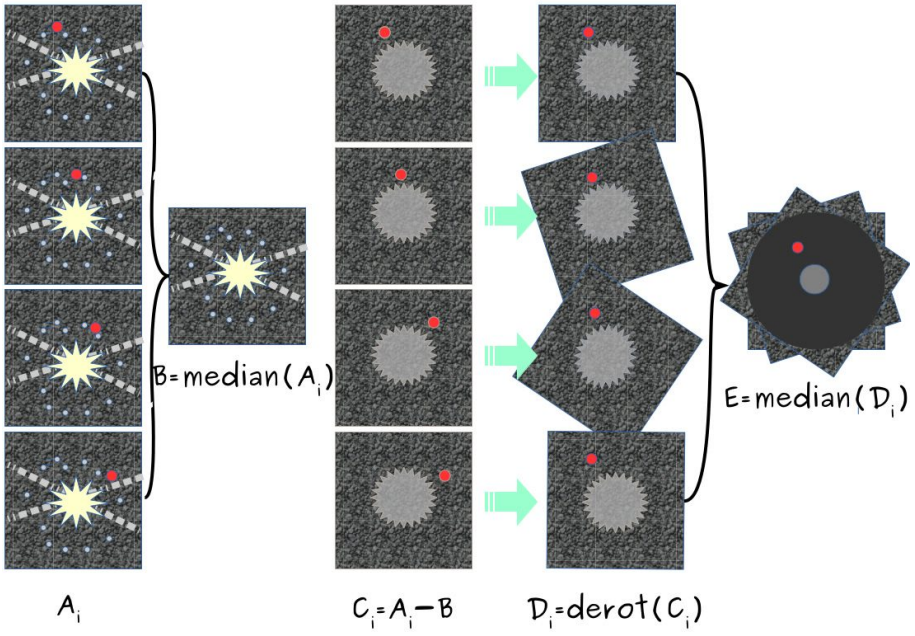

Figure 1. Graphical scheme of ADI technique (online image)

2.3 Self-subtraction factor

It is very important to stress out how important is to account for the planet self-subtraction factor. In fact, when the ADI or PCA were performed there is the risk of planet removal if the field rotation is small. This effect of course depends on the planet separation from the host star, the drop of its light is bigger at small separation and decreases at large separation. This is due to the fact that the same FoV rotation corresponds to a slower motion of the planet at small radial separations from the star, with respect to larger separations. This effect results in a subtraction of both speckles and the planet signal near to the star (Figure 2).

For a preliminary estimate of this effect, we generated a sequence of images containing some planets at different position angles, then we applied a simple ADI and PCA pipeline on it and we calculated the final residual signal at the known location of the planet. For the calculation, we assumed a 30 images sequence of 1 hour total duration, we chose two FoV rotation cases (30° and 90° rotation within 1 hour observation), according to the LBT object visibility (see Figure 3) and assuming the maximum possible value (at the moment of star culmination) in the middle of the time observation. In this way we want to emphasize the dependence of the self-subtraction effect with respect to the amount of the object rotation.

Figure 4 reports signal loss as a function of FoV rotation at different separations from the star for a sample of 30 simulated images. Near the host star ($< 400mas$) for a small FoV rotation (30°: black lines in the Figure 4) the self-subtraction of the planet light is more than 40% if the PCA algorithm is adopted, the ADI technique results less aggressive on the signal drop, and decreases from 40% to 10% in the small separation range. To obtain a decrease of the planet light less than 40% on whole separation ranges we need a wider FoV rotation, as large as 90 degrees (red lines in the Figure 4).
At small separation 90° of field rotation is necessary to preserve the highest level of light. According to our simplified model, to obtain such a rotation in 1 hour we need the target to be closer than 6° to the zenith. For preserving the same amount of the planet light for larger separations ($> 400mas$) a FoV rotation of 30° is sufficient and corresponds to an observed target farther than 20° to the zenith. The observation strategy looks to be very important, to allow the observation of every target of interest in optimal conditions as in maximum height on the horizon and for an exposure time such as to maximize the rotation angle of the planet.

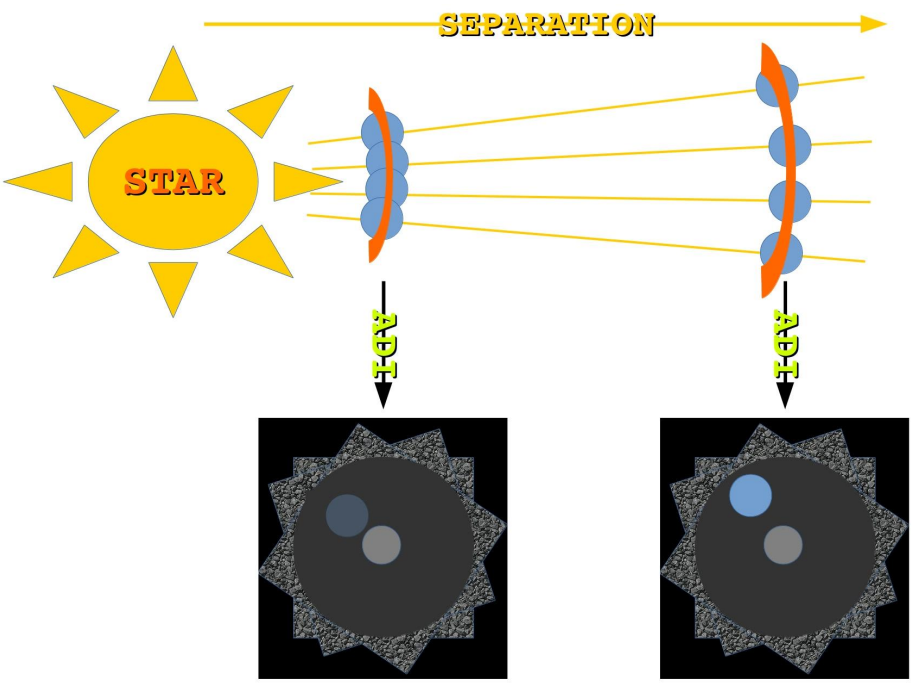

Figure 2. Graphic scheme of the self-subtraction effect depends on the separation from the host star

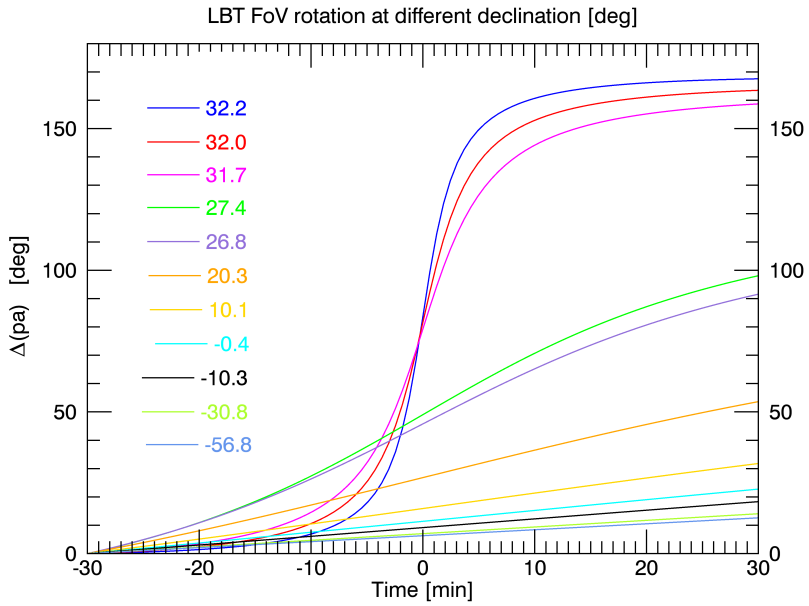

Figure 3. An example of parallactic angle values for objects at different declinations during an observation of 1 hour at LBT

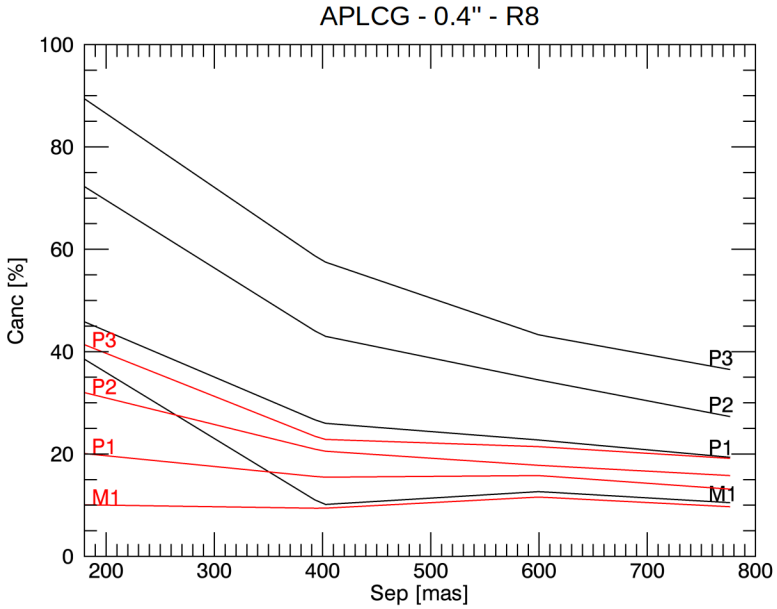

Figure 4. Amount of the planet light that is self-subtracted by the post processing reduction (M1 for simple ADI and P# for PCA with # of used modes) for APLCG coronagraph in a high Strehl condition. Black lines correspond to a 30° FoV rotation and the red ones to a 90° rotation

3. RESULTS

3.1 Faint end magnitude target

Performances in the low Strehl regimes are investigated. We simulated a sequence of 30 images of $1sec$ integration time each. The quasi-static speckles noise is $30nm\ rms$, while the applied residual jitter due to uncorrected vibrations is $3mas\ rms$. The same values have been used in all simulations showed in the following sections, unless otherwise specified.
The self-subtraction of the planet light as explained in Sec. 2.3 strictly depends on the FoV rotation and separation and in the following results we take it into account, that is the presented curves are already correct for the self-subtraction factor on the overall separation range.
Fig. 5, Fig. 6, Fig. 7 and Fig. 8 show raw contrast obtained with a Gaussian Lyot coronagraph for a star of magnitude $R = 10$ and $R = 12$ in different seeing condition. The Gaussian coronagraph has non-zero transmission inside the Inner Working Angle (IWA), so that it allows a performance estimation even at very small angular separations ($2\ \lambda/D$).
It is visible that observing faint objects the performances are not much sensible to the amplitude of the FoV rotation (the largest difference is of about a half of magnitude near the IWA in the case of an $R = 10$ star) independently of the simulated coronagraph and algorithm applied. On the contrary we will show in the next Section (3.2) a larger effect if we observe bright targets.

3.2 Bright end magnitude target

In Fig. 9, Fig. 10, Fig. 11 and Fig. 12 we show the results obtained with different coronagraphs in the case of a magnitude $R = 8$ target and 0.4" seeing value. We also analysed the performance in bad seeing condition (1") in Fig. 13, Fig. 14, Fig. 15 and Fig. 16.
The effect of the FoV rotation is stronger with respect to the faint case; in fact we gain more than one magnitude near the IWA and a half magnitude at $400mas$ for example with the SP coronagraph configuration in both seeing cases (0.4" and 1").

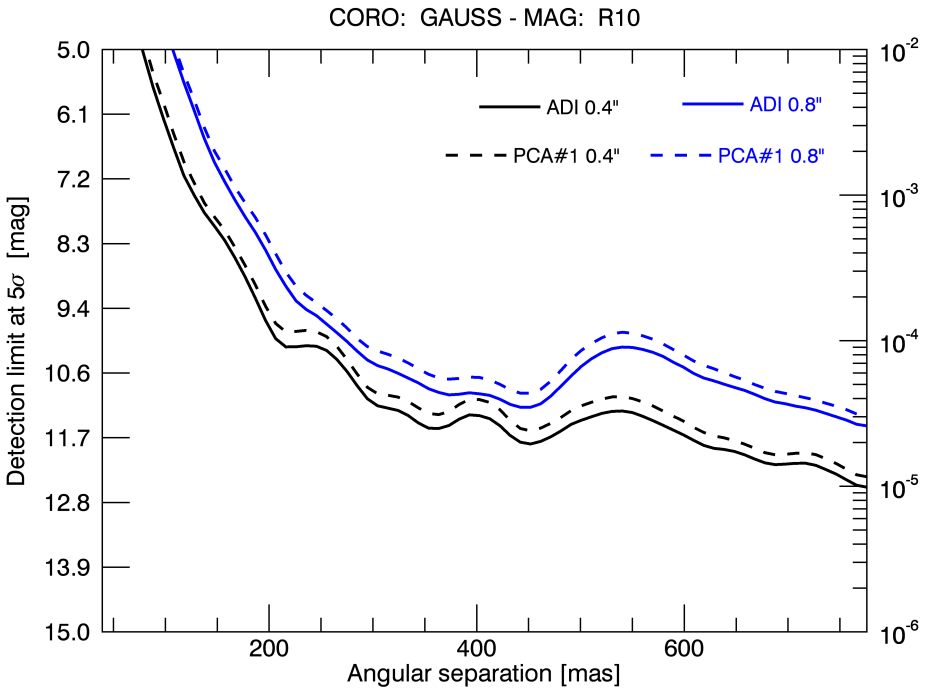

Figure 5. ADI and PCA performances for 30° of FoV rotation for a star of magnitude $R = 10$ in different seeing condition

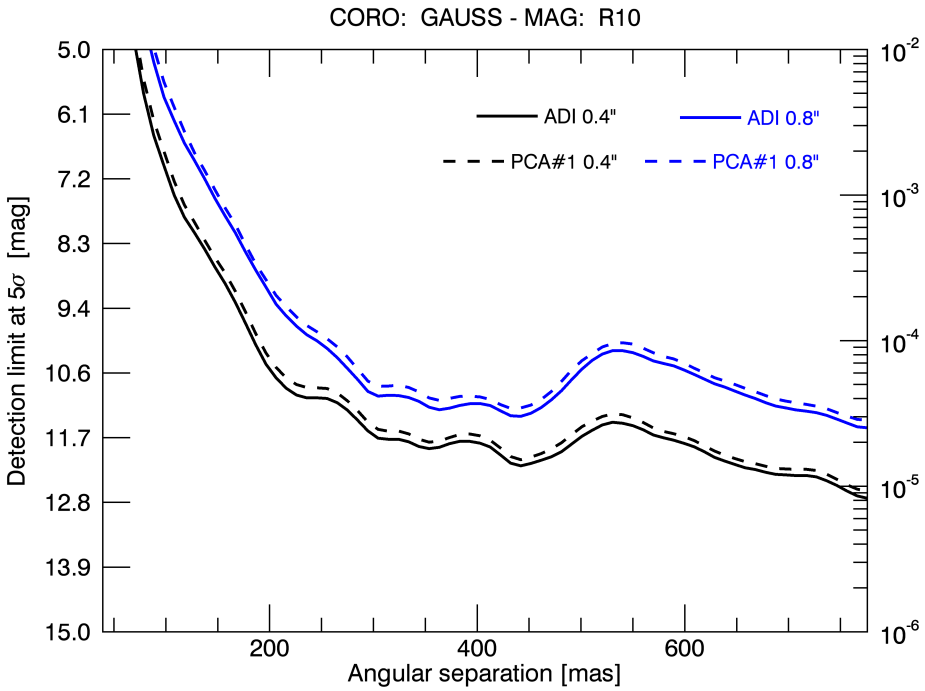

Figure 6. ADI and PCA performances for 90° of FoV rotation for a star of magnitude $R = 10$ in different seeing condition

3.3 Impact of number of images in the post processing

We started simulating data sequences as long as 100 images. According to theory,[12] higher noise attenuation occurs increasing the number of acquired images, up to a factor square root of N, where N is the total number of images. The cases of APLCG coronagraph is reported in Figure 17.

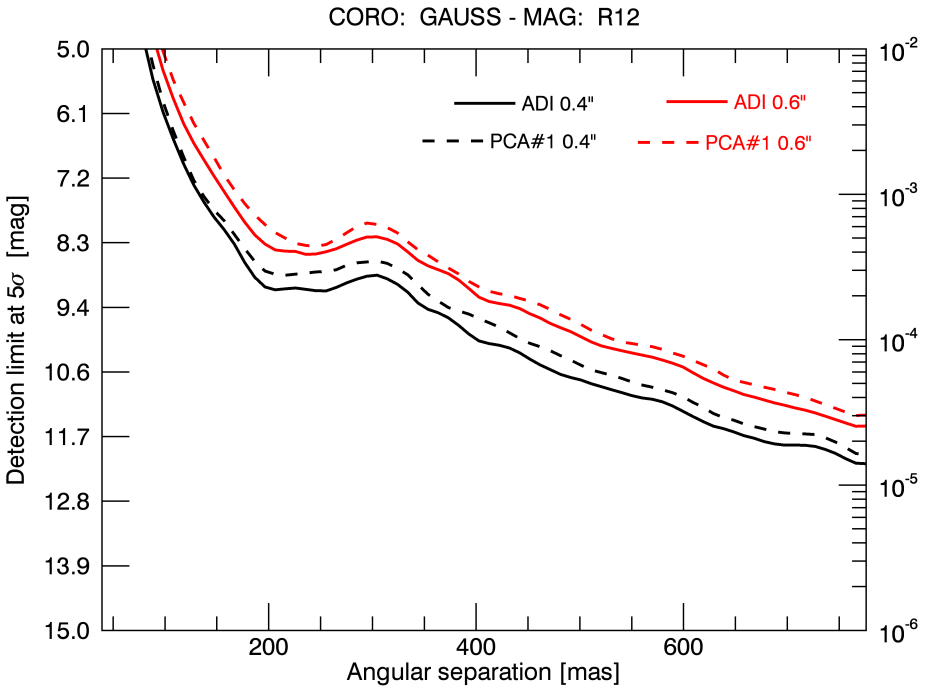

Figure 7. ADI and PCA performances for 30° of FoV rotation for a star of magnitude $R = 12$ in different seeing condition

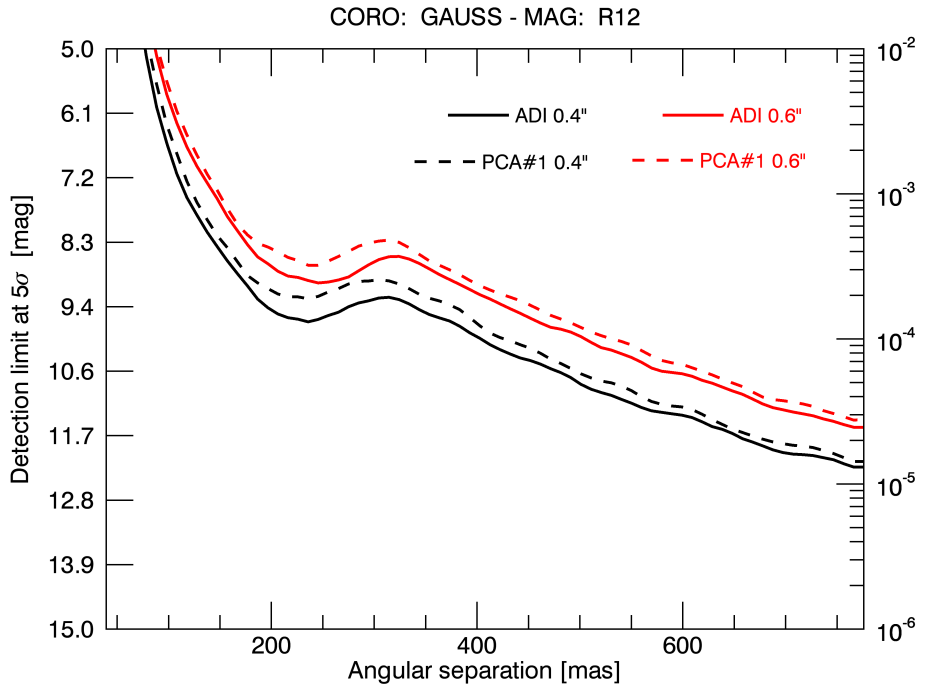

Figure 8. ADI and PCA performances for 90° of FoV rotation for a star of magnitude $R = 12$ in different seeing condition

A gain of more than one magnitude at all angular separations is obtained going from 30 to 100 images. As a comparison, SPHERE in Ref. [14] reaches 14 magnitudes of contrast at $400mas$ from the extreme bright star Sirius A. We also reported the results of two different FoV rotation angles to stress the importance of this effect, particularly at near separations from the host star.

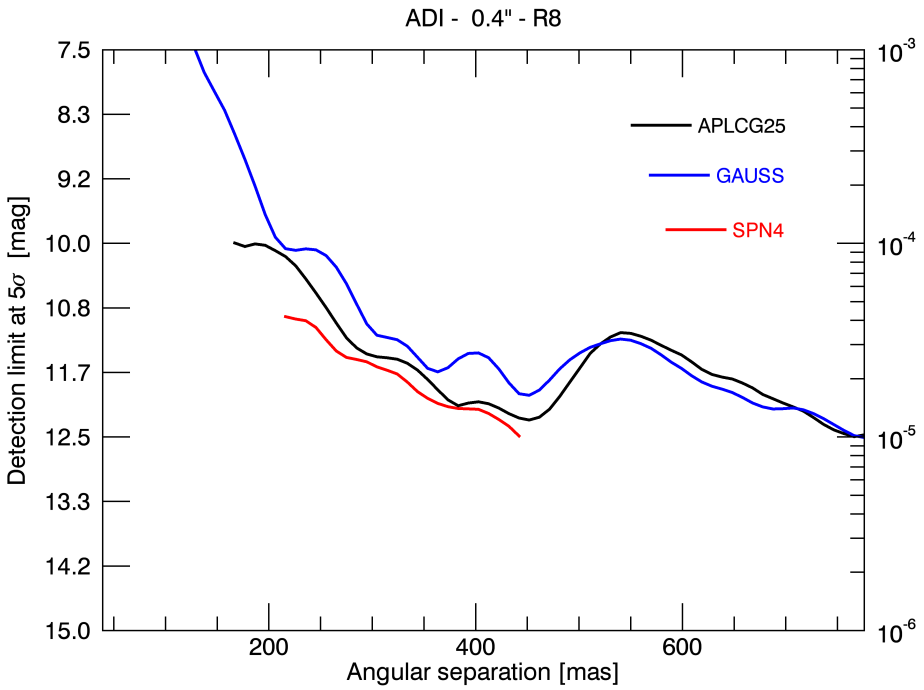

Figure 9. ADI performances for 30° of FoV rotation

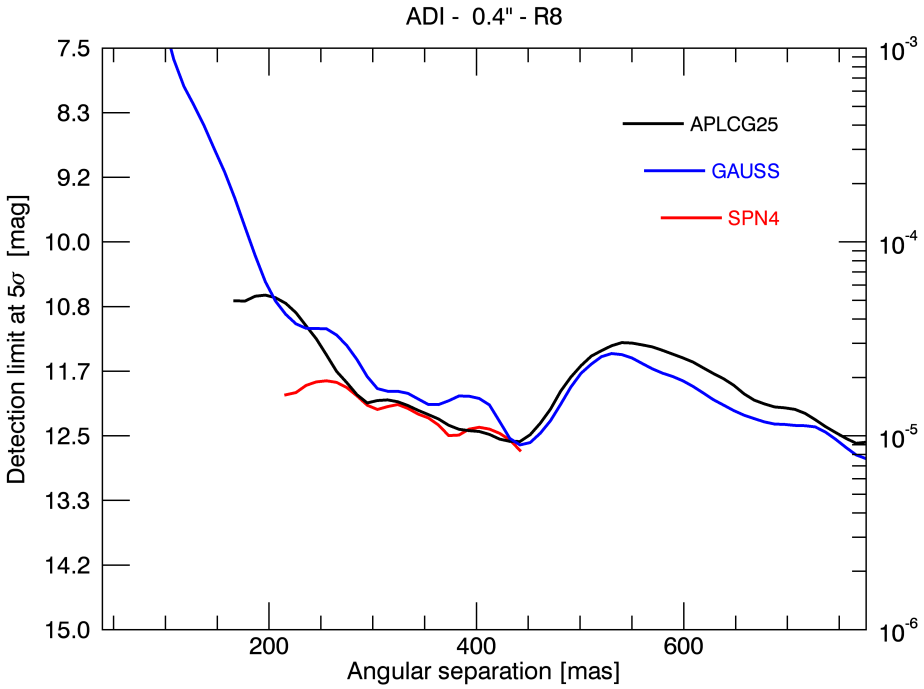

Figure 10. ADI performances for 90° of FoV rotation

4. CONCLUSIONS AND ON-GOING WORK

We have improved our simulations in many aspects, in particular with the introduction of speckle temporal evolution. As an indication that we are going in the right direction, a reasonable amount of quasi-static aberrations yields detection limits in good agreement with real on-sky SPHERE observations.

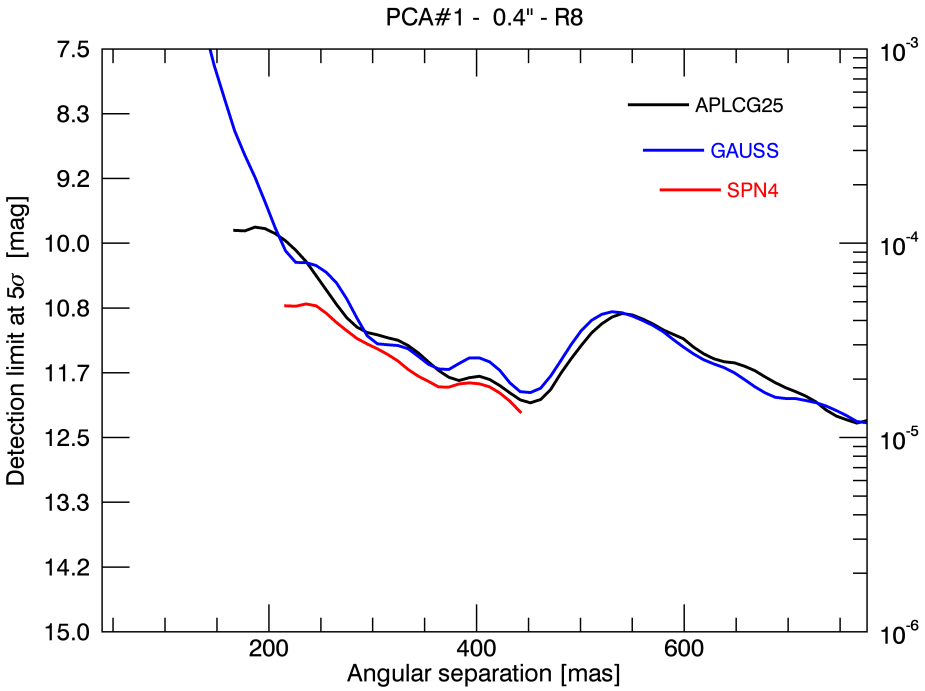

Figure 11. PCA performances for 30° of FoV rotation

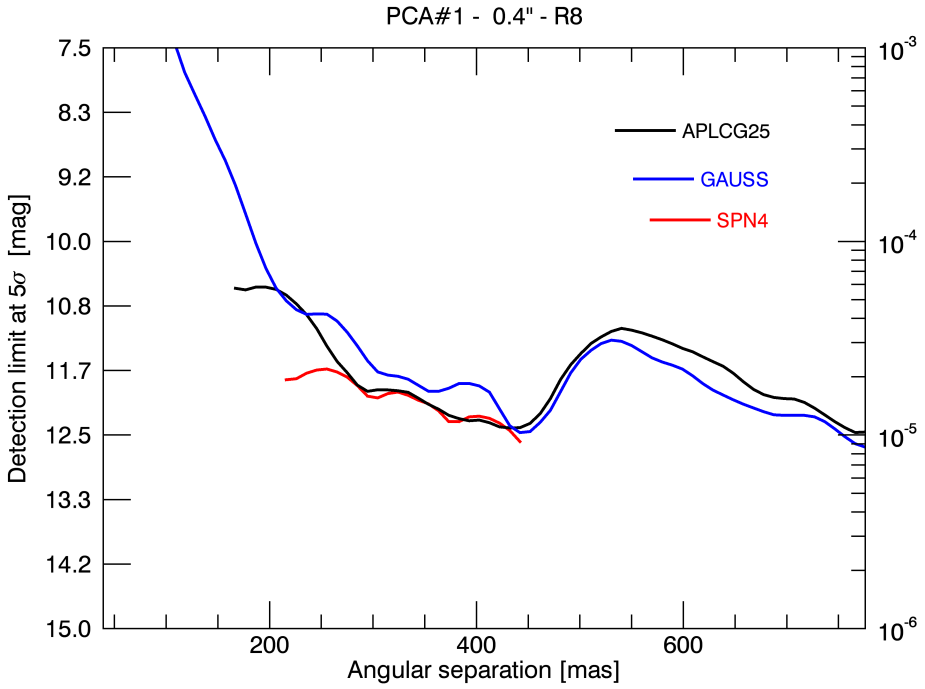

Figure 12. PCA performances for 90° of FoV rotation

Long ADI sequences are still difficult to generate because of computational time. We are focusing on increasing the number of images to compare our simulations to the real amount of data taken during an on sky observation and also because we are confident that the PCA performance will become more and more successful by using more images.

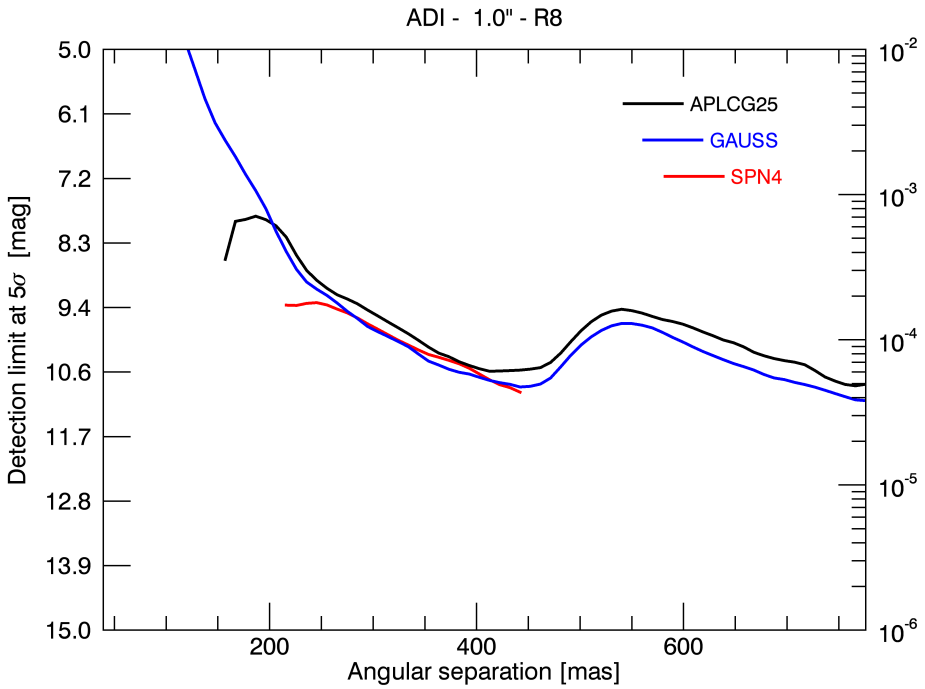

Figure 13. ADI performances for 30° of FoV rotation

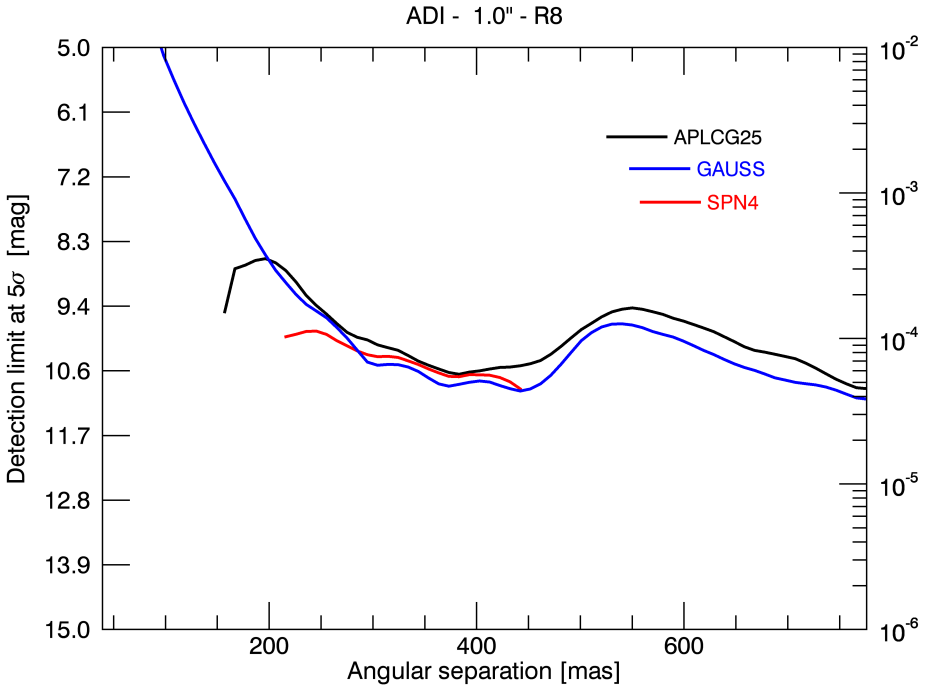

Figure 14. ADI performances for 90° of FoV rotation

At this stage of the analysis we noticed that a good observation strategy and the application of a solid reduction technique affects the instrument performance more of the coronagraph configuration, however some differences in the performance could be appreciated near the IWA by using the SP mask.
Furthermore a simple ADI algorithm seems to achieve better performance considering the self-subtraction factor,

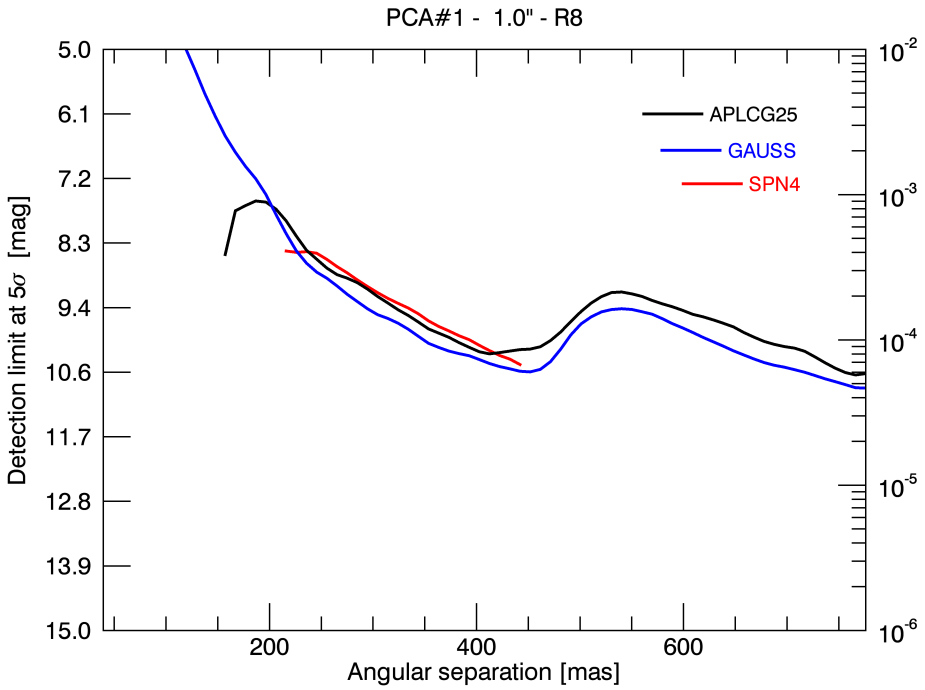

Figure 15. PCA performances for 30° of FoV rotation

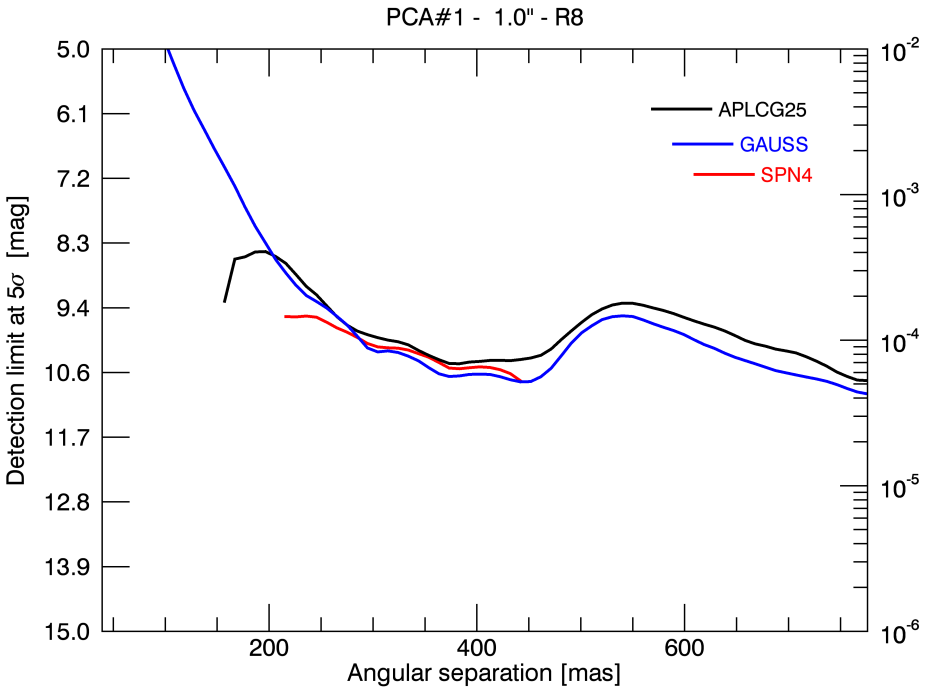

Figure 16. PCA performances for 90° of FoV rotation

in this way we are testing on 100 frames data-cubes the application of more than one median for the whole data set, by subdividing the simulated images in a number of subsets which are chosen by paying specific attention to preserve the light of the planet at different separations.

We are also investigating the effect of planet self-subtraction more in detail by injecting fake planets directly

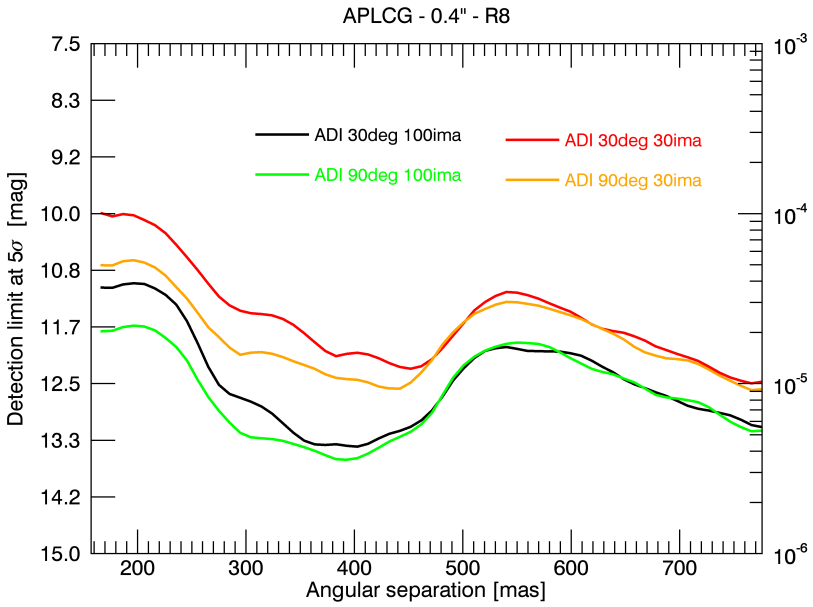

Figure 17. ADI algorithm on 30 and 100 simulated images for 30° and 90° of FoV rotation

into simulated sequences and by implementing an "ad hoc" code to find them by combining both ADI and PCA algorithms in synergy.

REFERENCES

[1] Schneider, J., "The extrasolar planets encyclopaedia." http://exoplanet.eu/catalog.php.

[2] Ren, D., Dou, J., Zhang, X., and Zhu, Y., "Speckle noise subtraction and suppression with adaptive optics coronagraphic imaging," *The Astrophysical Journal* **753**, 99 (2012).

[3] Wall, M. E., Rechtsteiner, A., and M., R. L., "Singular Value Decomposition and Principal Component Analysis," *ArXiv Physics e-prints* **http://adsabs.harvard.edu/abs/2002physics...8101W** (2002).

[4] Farinato, J., Baffa, C., Baruffolo, A., Bergomi, M., Carbonaro, L., Carlotti, A., Centrone, M., Codona, J., Dima, M., Esposito, S., Fantinel, D., Farisato, G., Gaessler, W., Giallongo, E., Greggio, D., Hinz, P., Lisi, F., Magrin, D., Marafatto, L., Pedichini, F., Pinna, E., Puglisi, A., Ragazzoni, R., Salasnich, B., Stangalini, M., Verinaud, C., and Viotto, V., "The NIR arm of SHARK: System for coronagraphy with High-order Adaptive optics from R to K bands," *International Journal of Astrobiology* **14**, 365–373 (2015).

[5] Hill, J. M. and Salinari, P., "Large Binocular Telescope project," *Proc. SPIE* **4004**, 36–46 (2000).

[6] Esposito, S., Riccardi, A., Pinna, E., Puglisi, A. T., Quirs Pacheco, F., Arcidiacono, C., Xompero, M., Briguglio, R., Busoni, L., Fini, L., Argomedo, J., Gherardi, A., Agapito, G., Brusa, G., Miller, D. L., Guerra Ramon, J. C., Boutsia, K., and Stefanini, P., "Natural guide star adaptive optics systems at LBT: FLAO commissioning and science operations status," *Proc. SPIE* **8447**, 84470U (2012).

[7] Vassallo, D., Carolo, E., Farinato, J., Bergomi, M., Bonavita, M., Carlotti, A., D'Orazi, V., Greggio, D., Magrin, D., Mesa, D., Pinna, E., Puglisi, A., Stangalini, M., Verinaud, C., and Viotto, V., "An extensive coronagraphic simulation applied to LBT," *This conference* (2016).

[8] Beuzit, J., Boccaletti, A., Feldt, M., Dohlen, K., Mouillet, D., Puget, P., Wildi, F., Abe, L., Antichi, J., Baruffolo, A., Baudoz, P., Carbillet, M., Charton, J., Claudi, R., Desidera, S., Downing, M., Fabron, C., Feautrier, P., Fedrigo, E., Fusco, T., Gach, J., Giro, E., Gratton, R., Henning, T., Hubin, N., Joos, F., Kasper, M., Lagrange, A., Langlois, M., Lenzen, R., Moutou, C., Pavlov, A., Petit, C., Pragt, J., Rabou, P., Rigal, F., Rochat, S., Roelfsema, R., Rousset, G., Saisse, M., Schmid, H., Stadler, E., Thalmann, C., Turatto, M., Udry, S., Vakili, F., Vigan, A., and Waters, R., "Direct detection of giant extrasolar planets with SPHERE on the VLT," *Astronomical Society of the Pacific workshop Proc.* **430**, 231 (2010).

[9] Lyot, B., "The study of the solar corona and prominences without eclipses," *Monthly Notices of the Royal Astronomical Society* **99**, 580 (1939).
[10] Soummer, R., "Apodized Pupil Lyot Coronagraph for Arbitrary Telescope Apertures," *The Astrophysical Journal* **618**, L161 (2005).
[11] Carlotti, A., Kasdin, N., Vanderbei, R., , and Delorme, J., "Optimized shaped pupil masks for pupil with obscuration," *Proc. SPIE* **8442**, 54 (2012).
[12] Marois, C., Lafreniere, D., Doyon, R., Macintosh, B., and Nadeau, D., "Angular Differential Imaging: A Powerful High-Contrast Imaging Technique," *The Astrophysical Journal* **641**, 556–564 (2006).
[13] Amara, A. and Quanz, S., "Pynpoint: an image processing package for finding exoplanets," *Monthly Notices of the Royal Astronomical Society* **427**, 948–955 (2012).
[14] Vigan, A., Gry, C., Salter, G., Mesa, D., Homeier, D., Moutou, C., and Allard, F., "High-contrast imaging of Sirius A with VLT/SPHERE: looking for giant planets down to one astronomical unit," *Monthly Notices of the Royal Astronomical Society* **454**, 129–143 (2015).